Appeared in *1999 ASME Wind Energy Symp,* 37th ASME/AIAA Annual Mtg.
Submitted for review, *Journal of Solar Energy,* ASME.

Moment-Based Load and Response Models with Wind Engineering Applications

Steven R. Winterstein and Tina Kashef
Civil and Environmental Engineering Dept., Stanford University

Abstract

A general method is shown here to model wind loads and responses for reliability applications. This method characterizes the short-term loads and responses by a few summary statistics: specifically, by a limited number of statistical moments. A suite of moment-based models are derived and applied here, illustrating how this statistical moment information can best be utilized. Two examples are shown: the fatigue analysis of a wind turbine component, and the vibration response of a fixed structure to nonlinear wind drag loads.

Introduction

As in other structural engineering applications, reliability analysis of structures subjected to wind requires careful study of appropriate load models. Whether these are based on imperfect analytical predictions or on incomplete field data, such load models can often be best described in a probabilistic manner. We illustrate here a general strategy to construct such models, based on load statistics available from analytical predictions or from limited data: specifically, from a limited set of statistical moments.

In general, it is convenient to identify two distinct time scales of load variation:

Short term behavior. Over short periods—e.g., over 10 minutes to several hours—it is reasonable to assume that global loads and responses exhibit a statistical steady-state condition. The resulting "short-term problem" is then to describe the probability distribution of these loads and responses during such a steady-state, in which the wind excitation is parameterized for example by the mean wind speed $\overline{V}$ and some measure I of turbulence intensity.

Long term behavior. Long-term modelling, and resulting reliability assessment, requires knowledge of how the probability distributions of loads/responses vary systematically over different wind conditions (e.g., over different values of mean wind speed $\overline{V}$ and turbulence intensity I). To study these systematic variations, it is convenient to represent these short-term load/response distributions parametrically, in terms of a few critical summary statistics. As noted above, these statistics are taken here to be a limited set of statistical moments (e.g., mean, standard deviation, skewness, etc.).

If this moment-based description is sufficiently informative, the long-term modelling step can be viewed as a form of system identification—in which a generally complex, nonlinear system is succinctly represented, for statistical analysis purposes, by its load/response moments as a function of wind excitation parameters such as $\overline{V}$ and I. Such system identification studies, of wind turbine load moments as functions of $\overline{V}$ and I, have recently been undertaken (e.g., Kashef and Winterstein, 1998). Our focus here is to consider and validate our focus on load moments; e.g., to study what information moments contain to predict full probability distributions, and how that moment information can best be used.

We show here a suite of general probabilistic models, which have been under ongoing development and refinement by the authors and their co-investigators at Stanford University. Each is designed to make best use of limited information; specifically, the first three or four statistical moments of the quantity of interest. Each of these is formed by constructing a mild polynomial transformation (quadratic or cubic) based on standard, well-established "parent" probability models. The choice between them is intended to reflect our engineering judgement as to a most appropriate parent

model. For example, an entire vibration time history may use a two-sided, Gaussian parent model, while if one instead has only a set of vibration ranges, a Weibull parent model may be most useful. Examples of both situations are shown here.

Typical probability models involve only one or two parameters, and hence can preserve only one or two statistical moments (e.g., mean and variance) of the observed variable. The resulting problem is that a number of plausible models, with very different tail behaviors and hence implied reliability levels, can often be fit to the same first two moments. This scatter in reliability estimates is said to be produced by *model uncertainty*. In particular, note that many common models of load amplitudes, for fatigue applications, include only one parameter; e.g., the Rayleigh and exponential models.

To lessen this model uncertainty, which is difficult to quantify, one is led to try to preserve higher moments as well. This will help to discriminate between various models, and hence reduce model uncertainty. This benefit does not come without cost, however: higher moments are more sensitive to rare extreme outcomes, and hence are more difficult to estimate from a limited data set. This is known as *statistical uncertainty,* which reflects the limitations of our data set.

Thus, our search for an "optimal" model reflects an attempt to balance between model and statistical uncertainties. Early practical experience (e.g., Winterstein, 1985; Winterstein, 1988) suggested that four moments are often sufficient when distorting a two-sided, Gaussian parent model to model an entire random vibration history. These have become known as "Hermite" models, because their quadratic and cubic terms are conveniently reorganized into Hermite polynomials when U is Gaussian (see also Lutes and Sarkani, 1997 for a review). Notably, a first-order Hermite model has recently been independently derived by P. Madsen, with an aim toward ultimate wind load estimation (Madsen et al, 1999).

Other recent studies have used cubic distortions of Gumbel models to represent extreme wave heights (Winterstein and Haver, 1991, Winterstein et al, 1995), and cubic distortions of Weibull models to estimate fatigue load ranges on wind turbines from limited field data (Winterstein and Lange, 1996, Winterstein et al, 1995). In this wind turbine case, we show here that simpler, quadratic Weibull models may be not only sufficient but superior. The reduced data needs of these three-moment models are particularly useful when predicting long-term fatigue damage, which requires load modelling across a range of wind conditions such as mean wind speed and turbulence intensity.

Scope and Organization

Our objectives here are two-fold. First, we offer a fairly comprehensive review of distribution modelling, statistical moments, and moment-based fitting. This review seeks to give a broad overview of these methods, as they have evolved over more than a decade of experience. This therefore involves a somewhat detailed look at their various implementations, presented for the first time in this unified way.

Our second objective is to illustrate the use of these models in several applications to wind engineering. Beyond showing how these models perform in specific situations, our goal is to indicate that the optimal use of these models (three- versus four-moment, Weibull vs normal parent model) is apt to be problem-specific. Those with more applied interests may wish to focus first on the examples, and refer back to the methodology section for supporting technical detail.

Methodology

Moments and Normalized Moments

Formally, the k-th moment of a random variable X can be defined as a weighted average in terms of its probability density $f(x)$:

$$\mu_k = E[X^k] = \int_{all\ x} x^k f(x) dx \qquad (1)$$

If limited sample data $x_1 ... x_n$ are available, one typically estimates μ_k as $\sum_{i=1}^{n} x_i^k / n$. When k=1 this returns the "mean value" of X, commonly denoted μ without numerical subscript.

Higher moments μ_2, μ_3, ... can also be calculated directly from Eq. 1. To facilitate interpretation and model fitting, however, it is common to report normalized versions of these higher moments. In particular, the second moment is commonly reported for the shifted quantity $X - \mu$:

$$\sigma^2 = E[(X-\mu)^2] = \int_{all\ x} (x-\mu)^2 f(x) dx \qquad (2)$$

Data-based estimates of σ^2, the *variance* of X, commonly follow a two-pass procedure: one first estimates μ from the sample average, then subtracts μ from each datum before estimating the second moment. This subtraction ensures that σ^2 will be invariant to arbitrary shifts in the original data set.

In a similar fashion, still higher moments are normalized by (1) shifting the data with respect to μ and (2) rescaling the data with respect to σ:

$$\alpha_n = E[(\frac{X-\mu}{\sigma})^n] = \int_{all\ x} (\frac{x-\mu}{\sigma})^n f(x) dx \qquad (3)$$

In particular, α_3 and α_4 are respectively called the skewness and kurtosis coefficients. Each of the α_n quantities are unitless, and are preserved if the data are both shifted and rescaled in arbitrary manner. In our experience, moments above α_4 are often of limited use, due to (1) their considerable statistical uncertainty when based on limited data; and (2) the difficulty in constructing sufficiently flexible functional forms to preserve such higher-order information, even if perfectly known, without inducing multiple modes and erratic tail behavior.

Three-Moment Models

As noted above, our strategy here is to adopt a smooth, theoretical distribution as a first approximation to X. We denote this "parent" variable as U, commonly normalized to be unitless (e.g., a normal distribution shifted and rescaled to have zero mean and unit variance, a Weibull distribution rescaled to have unit mean). We then seek to add a small quadratic correction ϵU^2 to reflect the skewness of the data:

$$Y = U + \epsilon U^2 \tag{4}$$

This leads to a unique relationship between ϵ and skewness α_3, from which ϵ can be found by trial and error. Finally, the unitless quantity Y can be rescaled and shifted to form the physical variable X, without altering the unitless α_3 parameter:

$$X = x_0 + \kappa Y \tag{5}$$

in which $\kappa{=}\sigma_X/\sigma_Y$ to preserve the variance of X, and $x_0{=}\mu_X - \kappa\mu_Y$ to preserve the mean of X.

Note that by solving in sequence for the unitless parameter ϵ, the rescaling parameter κ, and finally the shift parameter x_0, we restore the physical properties of X in a manner consistent with how our higher moments removed them. Significantly, this permits us to avoid the need to solve simultaneous equations for multiple model parameters. This leads to particularly robust model fitting routines, which have been implemented both in the stand-alone package `FITS` (Kashef and Winterstein, 1998) and in FORM application packages such as `FAROW` and `CYCLES` (e.g. Jha and Winterstein, 1997).

While Eqs. 4–5 comprise an attractively simple model, they fail to cover all practical situations of interest. In particular, to ensure a mild, monotonic variation of Y with U, we require ϵ in Eq. 4 to be positive. As a result, Eq. 4 broadens the distribution of U, and hence produces a skewness somewhat greater than that of U (and less than that of U^2). Thus, we apply Eq. 4 in cases when the skewness of the data, α_{3X}, *exceeds* the skewness α_{3U} of the parent variable U. When this condition does not hold, we interchange U and Y in Eq. 4:

$$U = Y + \epsilon Y^2; \quad \alpha_{3U} \geq \alpha_{3X} \tag{6}$$

In this case, the positive ϵ term serves to expand the actual distribution tails to match that of the parent variable U. We believe the choice between these dual models (Eq. 4 or Eq. 6) notably enhances modelling flexibility. In either case, Eq. 5 is finally used to recover the physical variable X.

Four-Moment Models

In the same way that a quadratic transformation of U can be found to preserve three moments of X, a cubic transformation can be sought to preserve four moments. Formally, the generalization again leads to a dual set of models, depending on whether the kurtosis, α_{4X}, of the data is greater or less than that of the parent variable:

$$Y = U + \epsilon_2 U^2 + \epsilon_3 U^3; \quad \alpha_{4X} \geq \alpha_{4U} \tag{7}$$

$$U = Y + \epsilon_2 Y^2 + \epsilon_3 Y^3; \quad \alpha_{4X} \leq \alpha_{4U} \tag{8}$$

We again recover X from the unitless variable Y through Eq. 5.

In practice, a major challenge in these four-moment models is that the higher moments, α_3 and α_4, each vary with changes in either ϵ_2 or ϵ_3. Thus, two simultaneous nonlinear equations must be solved for ϵ_2 and ϵ_3, with no assurance of solution uniqueness or existence. We have developed the routine `FITTING` (Winterstein et al, 1995), to estimate ϵ_2 and ϵ_3 by constrained optimization, minimizing errors in both skewness and kurtosis values, while requiring Eq. 7 or Eq. 8 to remain monotonic. These may be more numerically intensive, however, and less well suited to multiple calls in automated fitting routines. Simpler, analytical approximations to ϵ_2 and ϵ_3 have been developed for the important special case when U is a standard normal variable. These are reviewed further in Example 2.

Examples: Overview

These higher-moment models have been applied in various ways when studying time-varying load and response quantities. Specifically, the two examples invoke models over two different sampling time scales:

Example 1: X=randomly sampled load peak or range. For fatigue applications, load ranges are commonly identified by rainflow counting. Here, it is common to choose a standard Weibull model for U. It is often advantageous when used with fatigue loads

data, which are often synthesized to directly report histograms of rainflow ranges (as in Example 1).

Example 2: X=randomly sampled vibration history. The vibration history is commonly sampled at a regular time interval Δt. In this case, it is common to choose a standard normal model for the parent variable U. While this model applies directly to the history when sampled at an arbitrary time point, it can be used both to estimate fatigue and extreme, ultimate load levels (Winterstein, 1988). These models permit all of the data in a time history to be used—if they are available—and these moments may be less sensitive to uninteresting high-frequency, low-amplitude vibration cycles than the moments of rainflow-counted ranges. Another advantage of this model is that, as Example 2 shows, the necessary moments of the history may be estimated in some cases directly from theory (i.e., the differential equations of motion), without recourse to empirical data-based models. Similar models have found general use within the offshore community, for which response history moments are readily estimated from nonlinear, multi-degree-of-freedom diffraction models (Winterstein et al, 1994).

Example 1: Quadratic and Cubic Weibull Models of Fatigue Load Ranges

The Data

We consider here an observed data set of bending stresses, measured on a specific horizontal-axis wind turbine (HAWT). Only the "flapwise" bending mode (out of the plane of rotation) is considered here. The data represent a total of roughly 4 hours duration, constructed from pooling various shorter intervals during which wind conditions were similar. Further, since fatigue is the prime concern, the stress time histories were rainflow-counted to achieve a set of stress range amplitudes, which—in histogram form—comprise the basis of our data set.

Figure 1 shows such a histogram of these "normalized" stress amplitudes. (The units of these data are somewhat artificial, hence results should be interpreted in only a relative way across different cases and models.) As is typical of such cases, there are many thousands of small-amplitude, high-frequency cycles.

Note, however, that fatigue damage is commonly assumed to be proportional to some power of S—e.g., S^b where b is on the order of 6–9 for typical composite blade materials. Hence, these small-amplitude cycles are of little fatigue consequence. This fact is clearly

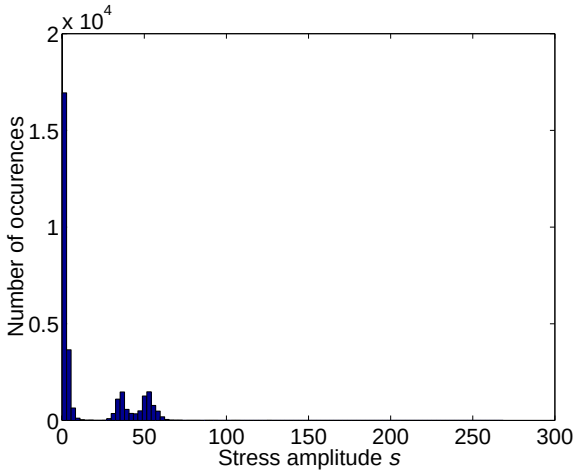

Figure 1: Histogram of rainflow-counted stress amplitudes, all values included.

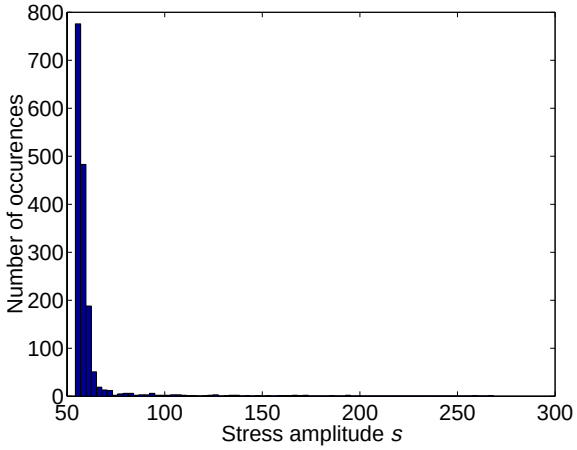

Figure 2: Histogram of rainflow-counted stress amplitudes, values above 54.2 only.

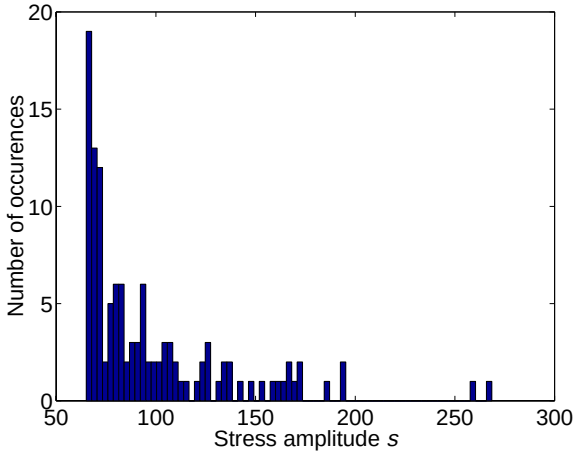

Figure 3: Histogram of rainflow-counted stress amplitudes, values above 65.1 only.

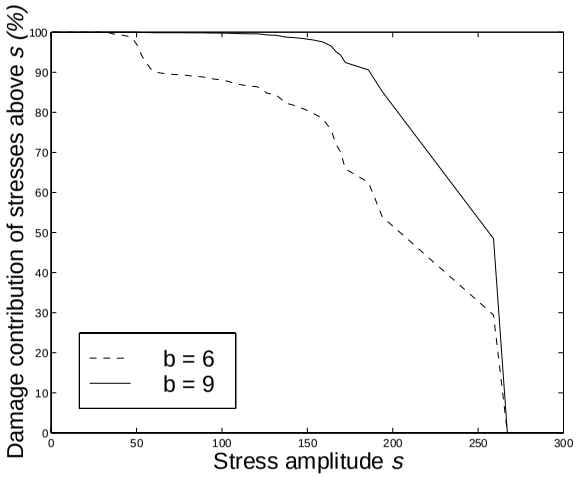

Figure 4: Contribution of different stress amplitude levels to total damage.

demonstrated in Figure 4 which shows the contribution of different stress amplitudes to the total damage for b values of 6 and 9. For such b values, direct estimates of S^b from the data would be very sensitive to rare extreme values and would not be sufficiently robust. we hope to avoid this problem by estimating S^b from a smooth distribution fitted to the first few moments of the data. The result, however, clearly depends on our choice of the distribution model. The greater importance of high-amplitude stresses in this context also makes tail behavior critically important when comparing different models, a point which general "goodness of fit" tests miss because they weigh all stress levels equally.

To focus modeling attention and data resources, we are therefore led to consider only stresses above a fixed threshold, here denoted σ_0. Figures 2 and 3 show such histograms for σ_0=54.2 and 65.1, respectively. While a general trend of exponential-like decay remains, focusing on higher thresholds permits greater scrutiny of the rare, high-amplitude stresses that govern fatigue damage.

At the same time, the higher thresholds leave us with an increasingly sparse data set, and hence considerable statistical uncertainty. We therefore investigate here whether a more general probabilistic model, such as the quadratic or cubic Weibull, can fit the data over a wider range than a simpler Weibull model with fewer parameters. If so, these more general models can be applied with a lower stress threshold, and hence retain a larger fraction of the original data set.

Below we compare the sensitivity of different Weibull models—when predicting maximum blade loads—to changes in the lower-bound stress threshold. The exceedence probabilities of models with different thresholds are not directly comparable, because they are conditioned upon different events. In other words, even though the exceedence probability of a level s is greater among stresses above a higher threshold, given the lower rate of occurrence of such stresses this will not necessarily translate into a higher predicted rate of occurrence of stresses greater than s. Consequently, models with different thresholds can only be compared using the implied probabilities of exceedence in fixed time intervals, rather than a fixed number of cycles.

Results I: Comparing Weibull and Quadratic Weibull Models

As the discussion above suggests, we may expect that a relatively simple model—here, the standard, two-parameter Weibull model—would behave acceptably, at least for a sufficiently high threshold. Figure 5 shows that for thresholds σ_0 at or above 54.2, the Weibull models do appear fairly satisfactory. For the lower threshold of σ_0=48.8, however, results deteriorate significantly. For example, the 10-hour load (hourly p=10^{-1}) appears to be underestimated by roughly one-third.

Figure 6 shows the same results as Figure 5, except that all results shown are now based on the quadratic Weibull model. The use of this more general model is shown to produce a notably more consistent fit across the range of data, even at the lowest threshold level σ_0=48.8. This supports the view, suggested above, that one may usefully extend these more general models farther back into the body of the loads distribution, and hence use a larger fraction of the data when estimating their parameters.

Results II: Comparing Quadratic Weibull and Cubic Weibull Models

Finally, we compare the quadratic Weibull models in `FITS`, as used to obtain the previous results, with similar results from the four-moment, cubic Weibull model implemented in the routine `FITTING`.

As its name implies, the cubic Weibull model (Eq. 7 or Eq. 8 with Weibull U) has a distribution function which, when plotted on ordinary Weibull scale, appears as a cubic polynomial. In the same way, the quadratic Weibull model (Eq. 4 or Eq. 6 with Weibull U) appears as a quadratic curve on this Weibull scale. Thus, unlike the quadratic Weibull model, the cubic Weibull distribution function may display a double curvature on Weibull scale. This may sometimes be a desirable capability, e.g., for two-sided phenomena whose left-

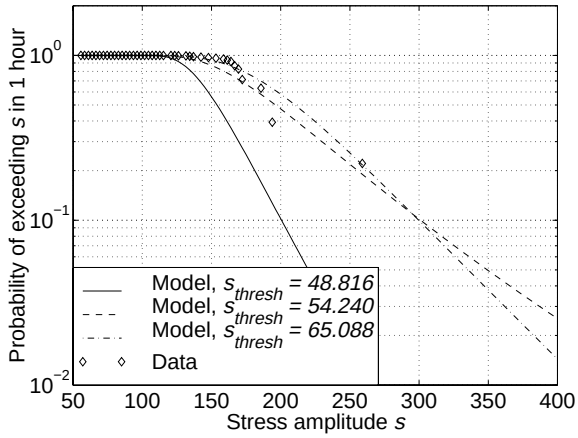

Figure 5: Fitting standard Weibull distributions, with various imposed shifts.

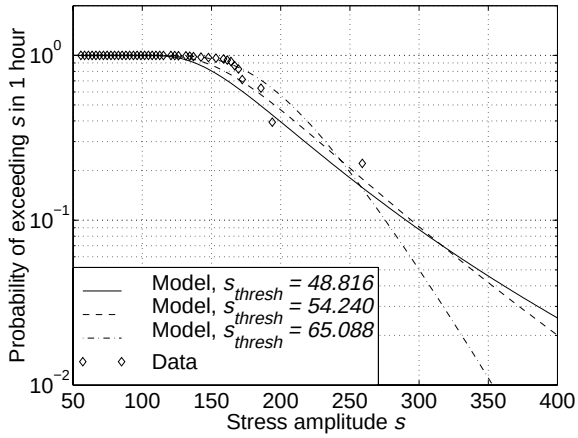

Figure 6: Fitting quadratic Weibull distributions, with various imposed shifts. (Note lesser sensitivity to shift value compared with standard Weibull fit.)

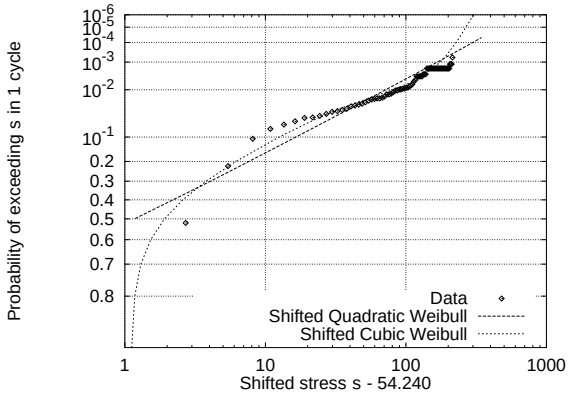

Figure 7: Quadratic vs. cubic Weibull blade load distributions, fit to values above 54.2 only. (Note the double curvature of cubic Weibull model on this Weibull scale plot.)

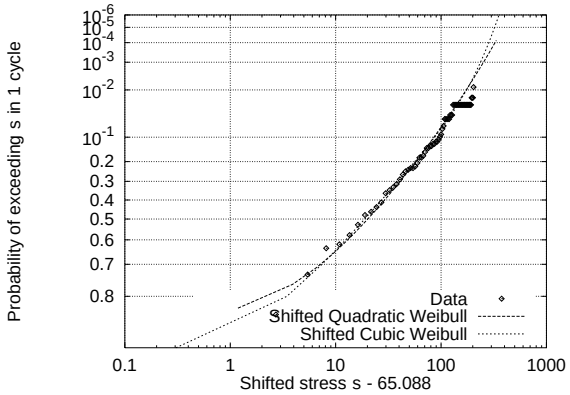

Figure 8: Quadratic vs. cubic Weibull blade load distributions, fit to values above 65.1 only.

and right-tail behaviors may differ. For variables such as load amplitudes, which have only a single (upper) tail, this flexibility may lead to overfitting.

Figure 7 shows that for this data set, the cubic Weibull model can display such double curvature. While one may debate whether the data show any such feature, it is fairly clear that extrapolating this highly nonlinear, doubly curved distribution function beyond the range of the data is potentially misleading. The quadratic Weibull appears to follow the trend of the data nearly as well over the range of the data, and by its nature permits a smoother, less tail-sensitive extrapolation beyond the highest data value.

As may be expected, Figure 8 shows that if we choose a sufficiently high threshold, the remaining data appear fairly homogeneous. Thus, in this case the cubic Weibull returns a rather similar result to the quadratic Weibull. (Still in this case, though, note the stronger curvature of the cubic Weibull beyond the last data point.) Indeed, even the standard Weibull may well suffice if only this upper tail is retained for the fit. These examples suggest, however, that the quadratic Weibull model permits a rather useful compromise: it is sufficiently flexible to model a wide range of the data set, yet is sufficiently constrained to retain fairly smooth, well-behaved extrapolation beyond the range of the observed data.

Example 2: Cubic Gaussian Models of Nonlinear Vibration

As a final example, we consider a general wind drag force applied to a fixed structure, such as a parked wind turbine. Adopting a simple 1DOF model of the response X:

$$m\ddot{X}(t) + c\dot{X}(t) + kX(t) = F_d(t) \tag{9}$$

in which the drag force, F_d, is given by

$$\begin{aligned} F_d(t) &= K_d[V(t) - \dot{X}(t)]^2 \\ &\approx K_d[V^2(t) - 2V(t)\dot{X}(t)] \end{aligned} \tag{10}$$

in terms of the incident wind velocity $V(t)$, the structural velocity $\dot{X}(t)$, and the effective drag coefficient K_d=$\rho C_d A/2$. The approximation in Eq. 10 assumes that $\dot{X}$ is relatively small compared with V. If we further approximate $V(t)\dot{X}(t)$ in this result by $\overline{V}\dot{X}(t)$ ($\overline{V}$=mean wind speed), this term can be viewed as an additional linear damping term, leading to a net damping coefficient c_{net}=$c + 2K_d\overline{V}$. Dividing Eq. 9 by m, we arrive at a normalized equation of motion with quadratic excitation:

$$\ddot{X} + 2\zeta\omega_n\dot{X} + \omega_n^2 X = Y(t)^2 \tag{11}$$

in which $Y(t)$ is a normalized wind velocity process, here assumed to be a Gaussian process.

We assume here that ω_n=1.26 [rad/sec], ζ=.30 (including viscous drag), and the covariance between $Y(t)$ and $Y(t+\tau)$ is $\exp(-0.12|\tau|)$. These parameter values are chosen to conform with a widely studied case in the random vibration literature (e.g., Kotulski and Sobczyk, 1981; Grigoriu and Ariaratnam, 1987). As noted in these references, the response moments are found to be α_{3X}=2.7 and α_{4X} = 14.3, quite far from their respective values (0 and 3) in the Gaussian case. In particular, moment-fit predictions for this model have been constructed based on maximum entropy principles. We therefore use this case to study the behavior of our moment-based models, and to compare these with the often cited maximum entropy results.

Four-Moment Hermite Model

Because we wish to model the vibration history X at an arbitrary time, we choose the parent variable U to be standard normal. It is convenient then to reorder terms in Eq. 7 in terms of Hermite polynomials. Combining this result with Eq. 5 yields

$$X = \mu_X + \kappa\sigma_X[U + c_3(U^2 - 1) + c_4(U^3 - 3U)] \tag{12}$$

in terms of the mean μ_X, standard deviation σ_X, and the normalizing constant

$$\kappa = (1 + 2c_3^2 + 6c_4^2)^{-1/2} \tag{13}$$

We then seek coefficients c_3 and c_4 for which the skewness and kurtosis of this model, $\alpha_{3,model}$ and $\alpha_{4,model}$, agree well with the true skewness α_{3X} and kurtosis α_{4X}. Formally, we may define an error $\Delta\alpha$ in matching these moments as a sum of squared deviations:

$$\Delta\alpha = [(\alpha_{3X} - \alpha_{3,model})^2 + (\alpha_{4X} - \alpha_{4,model})^2]^{1/2} \tag{14}$$

Results for c_3 and c_4 have been found to make $\Delta\alpha$ vanish to first-order (Winterstein, 1985) and second-order (Winterstein, 1988) in c_n. In particular, the first-order result is simply

$$c_3 = \frac{\alpha_{3X}}{6}; \quad c_4 = \frac{(\alpha_{4X} - 3)}{24} \tag{15}$$

A three-moment version of this result (with c_4=0) has been recently applied to model extreme wind turbine loads (Madsen et al, 1999). This three-moment version is attractively convenient, and may well suffice for some cases of extreme load estimation. It should not be used in more general cases (e.g., fatigue), in which both the upper and lower portions of the vibration cycle history are important. In this case the full four-moment model is needed to separately model and control the above-mean and below-mean behavior of the vibration history.

The most recent (and accurate) expressions have been fit to "exact" results from constrained optimization, which minimize $\Delta\alpha$ in Eq. 14 under the constraint that Eq. 12 remains monotonic (Winterstein et al, 1994):

$$c_3 = \frac{\alpha_{3X}}{6}\left[\frac{1 - .015|\alpha_{3X}| + .3\alpha_{3X}^2}{1 + 0.2(\alpha_{4X} - 3)}\right] \tag{16}$$

$$c_4 = c_{40}\left[1 - \frac{1.43\alpha_{3X}^2}{(\alpha_{4X} - 3)}\right]^{1 - 0.1\alpha_{4X}^{0.8}} \tag{17}$$

in which

$$c_{40} = \frac{[1 + 1.25(\alpha_{4X} - 3)]^{1/3} - 1}{10} \tag{18}$$

Note finally the convenience of Eqs. 12–18 as a *random vibration* model. If we assume that Eq. 12 relates a time-varying response $X(t)$ to a standard normal process $U(t)$ at each time t, we may directly apply the same transformation to other distributions arising from linear random vibrations; e.g., the Rayleigh distribution of peaks, first-passage results for global maxima,

etc. This approach has been used successfully in a number of nonlinear problems (Winterstein and Ness, 1989; Winterstein and Løseth, 1990; Winterstein et al, 1994).

Four-Moment Maximum Entropy Models

Two other four-moment models are commonly used. One is a polynomial distribution series; e.g., Charlier or Edgeworth. We omit these here, having done detailed comparisons that suggest they are limited to extremely mild non-Gaussianity (e.g., Winterstein, 1988). We do consider the second approach, which maximizes a quantity associated with the probability density $f_X(x)$ defined as "entropy" (Jaynes, 1957). The result, assuming four moments are known, is of the form

$$f_X(x) = \exp(-u(x)); \quad u(x) = \sum_{n=0}^{4} \lambda_n x^n \qquad (19)$$

A numerical algorithm is used to find constants $\lambda_1 ... \lambda_4$ that preserve (or minimize error in) the four moments. Unit area is achieved through λ_0. Note the similarity between Eq. 19 and Eq. 8 when U is Gaussian. Both ensure narrower-than-Gaussian ("hardening") behavior in the limit: $\lambda_4 > 0$ in Eq. 19 to achieve a proper pdf, and hence its distribution tails are ultimately narrower than the normal pdf $f_U(u)$. We may thus expect similarly successful results from Eqs. 8 and 19 for narrower-than-Gaussian distributions; e.g., if $\alpha_{4X} < 3$, the kurtosis of the Gaussian model. Eq. 19 is shown below to be somewhat less successful for softening cases ($\alpha_{4X} > 3$), compared with Eq. 12.

Numerical Results

Figure 9 shows the distribution of X, estimated by simulation, on normal probability scale. This figure also shows a Gaussian model, fit to m_X and σ_X. As expected, a two-moment Gaussian fit appears as a straight line on this scale; in addition, it dramatically underestimates response fractiles x_p at levels of practical interest (e.g., p above .99). The cubic Gaussian model is a marked improvement, showing good agreement far into the response tails. In contrast, the maximum entropy tail behavior is found inconsistent, due to its ultimate hardening nature noted above. It thus underestimates response fractiles x_p systematically for p above .999; compensating errors occur at lower fractiles in its effort to preserve moments through an inconsistent functional form. As might be expected, similar though somewhat less dramatic effects are found when

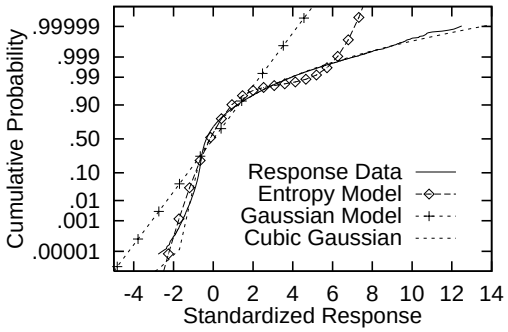

Figure 9: Oscillator Response; 30% Damping.

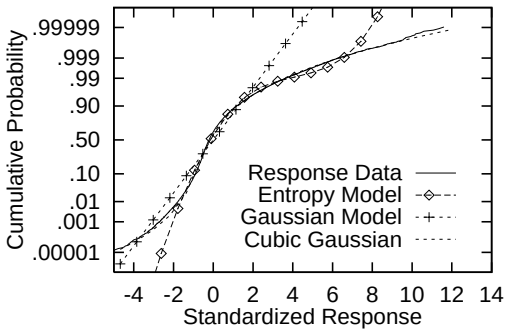

Figure 10: Oscillator Response; 10% Damping.

the damping is reduced to ζ=.10 (Figure 10), as the response becomes more nearly Gaussian.

Summary and Conclusions

- A general method is shown here to model wind loads and responses for reliability applications. This method characterizes the short-term loads and responses by a few summary statistics: specifically, by a limited number of statistical moments. A suite of moment-based models are derived and applied here, illustrating how this statistical moment information can best be utilized. For this modelling purpose, a set of moment-based probability models have been introduced and demonstrated. These use mild perturbations, in the form of quadratic or cubic transformations, of well-established "parent" probability models such as a Gaussian model of random vibration, or a Weibull model of its local ranges. Examples of both situations are shown here.

- An application to model load ranges of wind turbine blades is shown. A four-moment model established previously (Winterstein and Lange, 1996) is applied. Notably, simpler three-moment quadratic Weibull models are found here to be not only sufficient but superior. The reduced data needs of these three-moment models are particularly useful when predicting long-term fatigue damage, which requires load modelling across a range of wind conditions such as mean wind speed and turbulence intensity.

- An application to model random vibration response to nonlinear wind drag loads is also demonstrated. Here a four-moment ("Hermite") transformation of a Gaussian random process is shown to accurately follow the rather severe non-Gaussian behavior in these cases (e.g., α_{3X}=2.7 and $\alpha_{4X} = 14.3$, compared with the values 0 and 3 in the Gaussian case.) In contrast, the commonly used maximum entropy model is unable to accurately follow this trend in non-Gaussian behavior (Figures 9–10).

Acknowledgements

First, we gratefully acknowledge David Malcolm for providing us with loads data from a prototype horizontal-axis wind turbine. We also wish to thank Bill Holley and Paul Veers for their comments and contributions to this work. In addition, we acknowledge past Stanford researchers integrally related to the development of our statistical analysis methods, including Clifford Lange, Alok Jha, and Satyendra Kumar. Finally, this work is supported by the Wind Energy Program of the U.S. Department of Energy, through Sandia National Laboratories.

References

Grigoriu, M. and S.T. Ariaratnam (1987). Stationary response of linear systems to non-gaussian excitations. *Proc., ICASP-5,* ed. N.C. Lind, Vancouver, B.C., **II**, 718–724.

Jaynes, E.T. (1957). Information theory and statistical mechanics. *Phys. Rev.*, **106**, 620–630.

Jha, A.K. and S.R. Winterstein (1997). *Cycles 2.0: Fatigue reliability models and results for wave and wind applications,* Rept. RMS–27, Reliability of Marine Structures Program, Dept. of Civ. Eng., Stanford University.

Kashef, T. and S.R. Winterstein (1998). Relating turbulence to wind turbine blade loads: parametric study with multiple regression analysis. Proc., 1998 ASME Wind Energy Symposium, 36th AIAA Aero. Sci. Mtg., 273–281.

Kashef, T. and S.R. Winterstein (1998). *Moment-based probability modelling and extreme response estimation: The FITS routine,* Rept. RMS–31, Reliability of Marine Structures Program, Dept. of Civ. & Environ. Eng., Stanford University.

Kotulski, Z. and K. Sobczyk (1981). Relating turbulence to wind turbine blade loads: parametric study with multiple regression analysis. *Journal of Statistical Physics*, **24**(2), 359–373.

Lutes, L.D. and S. Sarkani (1997). *Stochastic analysis of structural and mechanical vibrations,* Prentice-Hall.

Madsen, P.H., K. Pierce and M. Buhl (1999). Predicting ultimate loads for wind turbine design. *Proc., 1999 ASME Wind Energy Symposium,* 37th AIAA Aero. Sci. Mtg., to appear.

Winterstein, S.R. (1985). Nonnormal responses and fatigue damage. *J. Engrg. Mech.,* ASCE, **111**(10), 1291–1295.

Winterstein, S.R. (1988). Nonlinear vibration models for extremes and fatigue. *J. Engrg. Mech.,* ASCE, **114**(10), 1772–1790.

Winterstein, S.R. and C.H. Lange (1996). Load models for fatigue reliability from limited data. *Journal of Solar Energy*, Trans. ASME, **118**(1), 64–68.

Winterstein, S.R. and O.B. Ness (1989). Hermite moment analysis of nonlinear random vibration. *Computational mechanics of probabilistic and reliability analysis,* ed. W.K. Liu and T. Belytschko, Elme Press, Lausanne, Switzerland, 452–478.

Winterstein, S.R. and R. Løseth (1990). Jackup structures: nonlinear forces and dynamic response. *Proc., 3rd IFIP Conf. on Reliability and Optimization of Structural Systems,* Berkeley, CA.

Winterstein, S.R. and S. Haver (1991). Statistical uncertainties in wave heights and combined loads on offshore structures. *J. Offshore Mech. Arctic Eng.,* ASME, **114**(10), 1772–1790.

Winterstein, S.R., C.H. Lange, and S. Kumar (1995). *FITTING: A subroutine to fit four moment probability distributions to data,* Rept. SAND94-3039, Sandia National Laboratories.

Winterstein, S.R., T.C. Ude and G. Kleiven (1994). Springing and slow-drift responses: predicted extremes and fatigue vs. simulation. *Proc., BOSS-94,* **3**, Massachusetts Institute of Technology, 1–15.

Winterstein, S.R., T.C. Ude and T. Marthinsen (1994). Volterra models of ocean structures: extreme and fatigue reliability. *J. Engrg. Mech.,* ASCE, **120**(6), 1369–1385.